

PATENT REVIEW OF MINIATURE CAMERA LENSES
AND
A BRIEF COMPARISON OF TWO RELATIVE DESIGN PATTERNS

by

Luxin Nie

A Report Submitted to the Faculty of the

COLLEGE OF OPTICAL SCIENCES

In Partial Fulfillment of the Requirements

For the Degree of

MASTER OF SCIENCE

In the Graduate College

THE UNIVERSITY OF ARIZONA

2017

STATEMENT BY AUTHOR

The master's report titled *Patent Review of Miniature Camera Lenses and a Brief Comparison of two Relative Design Patterns* prepared by *Luxin Nie* has been submitted in partial fulfillment of requirements for a master's degree at the University of Arizona.

Brief quotations from this report are allowable without special permission, provided that an accurate acknowledgement of the source is made. Requests for permission for extended quotation from or reproduction of this manuscript in whole or in part may be granted by the copyright holder.

SIGNED: *Luxin Nie*

APPROVAL BY REPORT ADVISOR

This report has been approved on the date shown below:

<hr/>	<u>Nov 29, 2017</u>
<i>José M. Sasián</i>	Date
<i>Professor of Optical Sciences</i>	
<i>Professor of Astronomy</i>	

ACKNOWLEDGEMENTS

I would like to thank my family for their consistent support.

I would like to thank Prof. José Sasián for his beneficial advices in writing this report, his enlightening teaching in optics without reservation, and his life-changing influence of living as an ideal lens designer.

I would also like to thank my committee, Dr. Jim Schwiegerling and Dr. Dae Wook Kim. Their enthusiasm and devotion in education are very respectable and make me thankful.

Thank other professors, staffs and classmates. They together make the experience of studying in OSC enjoyable and unforgettable.

TABLE OF CONTENTS

Abstract	7
Patents Review	8
Representative Patterns	13
A Quick Evaluation	16
Two Relative Designs	19
Four Parameters Evaluation	20
RMS Wave-front Error As Criterion	23
Tolerancing By Element	26
Monte Carlo Analysis	28
Conclusions	31
References	33

LIST OF FIGURES

Fig. 1 Numbers of patent publication in different years	9
Fig. 2 Element number changing of miniature lenses over years	10
Fig. 3 Focal length changing of miniature lenses over years	11
Fig. 4 $F/\#$ changing of miniature lenses over years	12
Fig. 5 FOV changing of miniature lenses over years	13
Fig. 6 (a) Parameters W and S of sixteen lenses in Table 1	18
Fig. 6 (b) Parameters CS and AS of sixteen lenses in Table 1.....	18
Fig. 7 (a) Layout of the selected 6-element lens	19
Fig. 7 (b) Layout of the selected 7-element lens	19
Fig. 8 Parameter w of each element of two compared lenses	21
Fig. 9 Parameter $(cs + as) / 2$ of each element of two compared lenses	23
Fig. 10 RMS wave-front errors over HFOV	24
Fig. 11 (a) Histogram of RMS changes at center field	29
Fig. 11 (b) Histogram of RMS changes at zonal field	29
Fig. 11 (c) Histogram of RMS changes at edge field	30

LIST OF TABLES

Table 1 Representative design patterns of different element numbers	14
Table 2 Four parameters of the two compared lenses	20
Table 3 Selected field points and the local RMS values	25
Table 4 RMS changes of different perturbances at three field points	27
Table 5 Mean and standard deviation of Monte Carlo Analysis	30

ABSTRACT

The market share of mobile terminals, such as PC, smart phone, and tablet, increases rapidly in recent years. As a consequence, high-quality but low-cost compact camera modules for these platforms are in a great demand as well. Therefore, a large number of miniature camera lenses are designed and their patents are published. In this report, about 750 U.S. patents of miniature camera lenses are reviewed and the trend of their evolution is revealed. Then, sixteen representative designs are tabulated, and a quick evaluation on them is made to tell the optimums. Finally, two relative designs are selected and the tolerancing sensitivity on particular elements is studied.

Patents Review

Time span of the reviewed U.S. patents is from 2000 to 2017. Nearly all of them are assigned to five leading companies, namely Largan Precision Co., Kantatsu Co., Genius Electronic Optical Co., Fujifilm Co., and Samsung Electro-Mechanics Co., in the field of designing, manufacturing, and producing compact camera modules for mobile devices.

In each patent document, besides the **Date of Patent**, there is also a **Prior Publication Data**, where its prior publication date can be found. This date can be regarded as the first time an invention or design being publicized in the U.S. For example, the patent (**Patent No.:** *US 9,733,454 B2*. **Date of Patent:** *Aug. 15, 2017*.) has a **Prior Publication Data:** *US 2016/0170184 A1 Jun. 16, 2016*. Then, June 16th in 2016 was the first time this patent application being publicized in U.S., though it didn't formally become a patent until Aug. 15, 2017. In this report, each time related study uses this date as the time factor.

Fig. 1 is the numbers of patent publication in each year over the past two decades. We can see that the trend starts to speed up in 2012. About 160 patents were published in 2015, which makes it the bumper harvest year. The second summit came in 2014, which has about 130 patent publications. The patents in 2014 and 2015 share about 38.6% of the total. The year 2012, 2013, and 2016 together make about 31.3% of the total amount. However, the numbers in 2016 and 2017

are incomplete, since many designs initially published in these two years will not formally become U.S. patents until some years later and thus are not counted. In a short word, before 2016, the patent publication in the field of miniature camera lenses started to boom in 2012 and came to its summit in 2015.

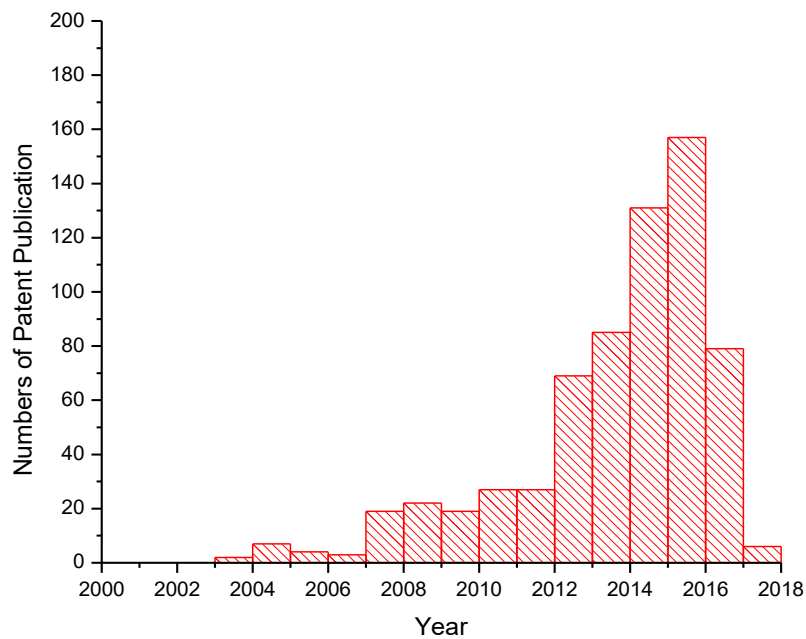


Fig. 1 Numbers of patent publication in different years

Camera lenses commonly have more than one element to make good imaging performance, like balancing aberrations, and so do miniature camera lenses. More elements usually mean more degrees of freedom to make a better design. Due to the advances in technique of polymer materials and injection modeling, adoption of non-traditional materials and aspherical elements becomes common, and even strengthens this advantage. In Fig. 2, the number of elements adopted in each

design is plotted. Powerless elements like IR filter are not counted.

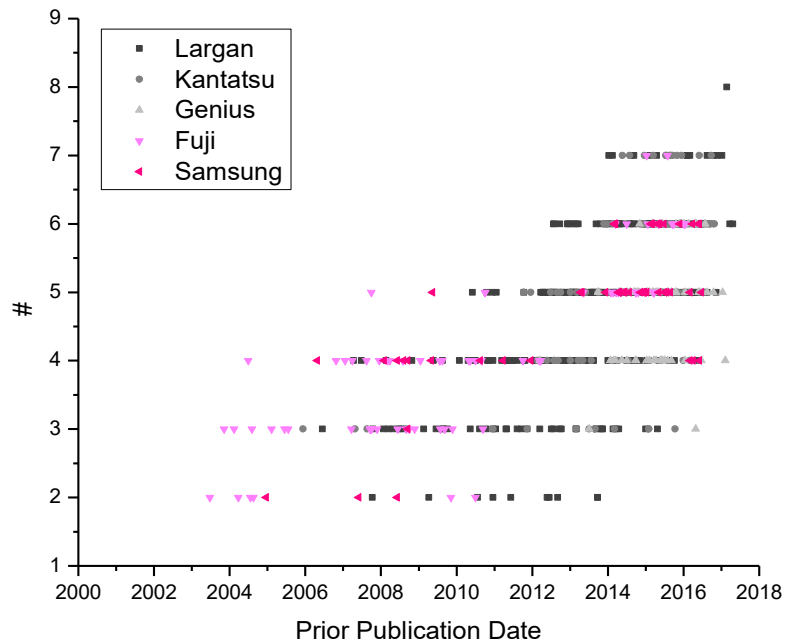


Fig. 2 Element number changing of miniature lenses over years

Three- and four-element patterns seem to be classical. They appeared almost at the early stage of miniature camera lens design and have thrived up till now. Both of the two patterns balance the requirements of good performance, robustness, and easy manufacture well, which makes them long-lasting over the past twenty years, and probably in the future.

Five-element pattern largely emerged in 2011, followed by six-element pattern arising in 2013, and seven-element pattern boomed one year later, in 2014. This trend reflects that due to largely reduced cost and highly improved assembling

technique, the pursuing of versatile performance starts to dominate.

Focal length is one of the most important parameters of lenses. It determines many imaging properties of lenses and is always first given. As plotted in Fig. 3, the distribution of focal length over publication year doesn't show any obvious preference. The value distribution of focal length is around 4 millimeters. This promises an appealing small thickness in modern slim electronic devices.

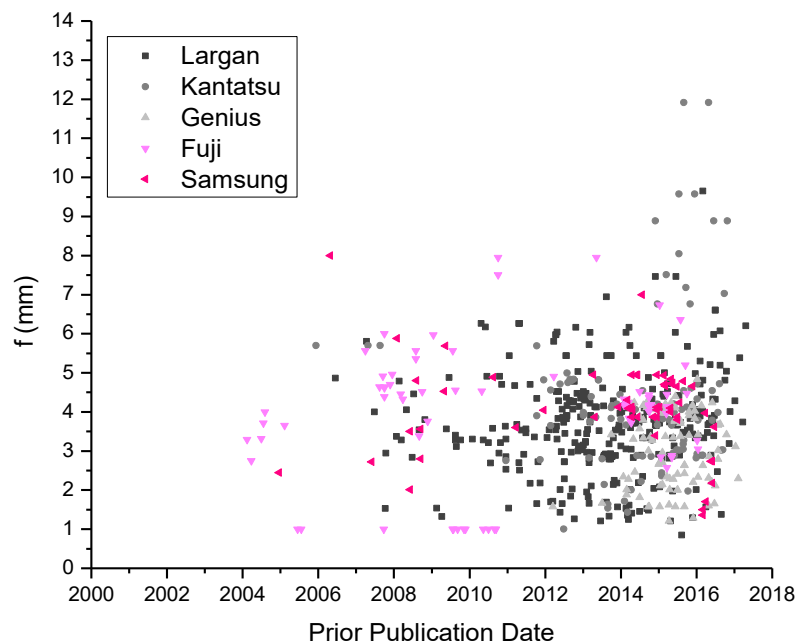


Fig. 3 Focal length changing of miniature lenses over years

Unlike focal length, the distribution of F-number ($F/\#$) over publication year in Fig. 4 demonstrates an obvious decreasing trend. $F/\#$ is related to the “speed” of a lens. Current miniature camera lenses have smaller $F/\#$, and thus are “faster”

than they used to be. “Fast” camera lenses usually have better performance in imaging moving object. Given that the application scenes of modern mobile devices are often in sport and video recording, this trend of F/# changing is reasonable.

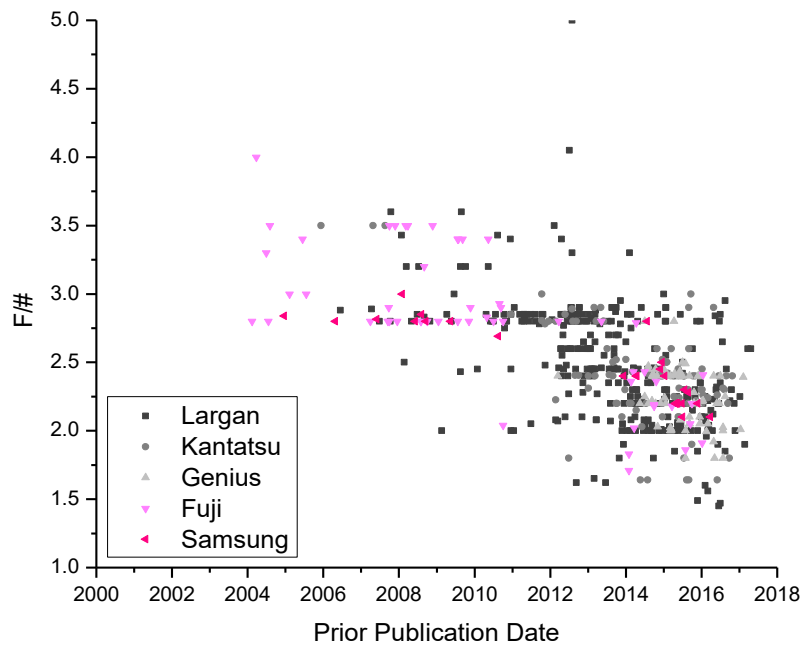


Fig. 4 F/# changing of miniature lenses over years

Another important lens parameter is field of view (FOV, HFOV for half FOV). Fig. 5 demonstrates the trend of FOV changing. The average of FOV over past twenty years increases slightly from about 60 to 70 degrees. However, the value range of FOV diverges with respect to years. Newly designed miniature camera lenses have various FOVs. This is probably a response to more diverse usage requirements in nowadays consumer electronics market, like a wide-angle lens in

a dual-lens module.

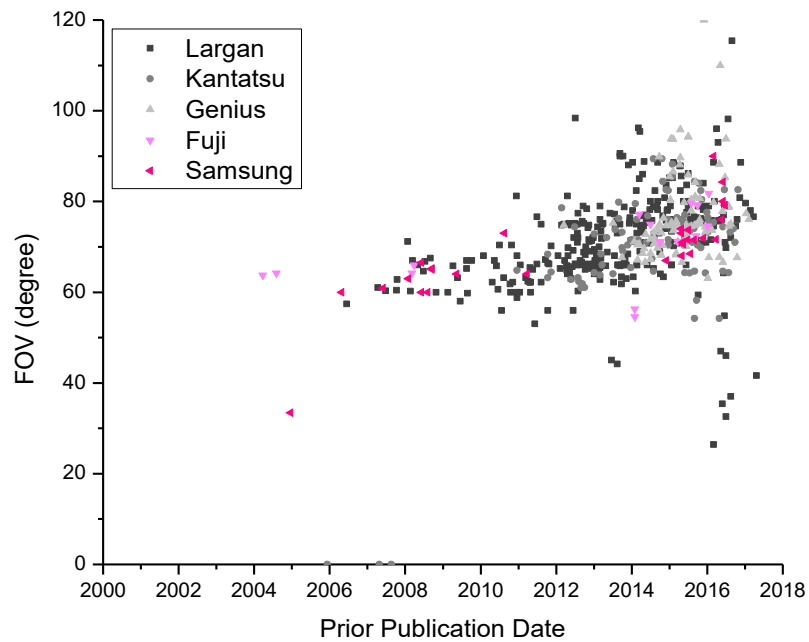


Fig. 5 FOV changing of miniature lenses over years

Representative Patterns

After some statistics, the evolution of design patterns is also interested. Some representative patterns with three, four, five, six, seven or even eight elements are shown in Table 1. Many other designs are varieties of them or got by shifting the stop.

Whatever the type of design, it is obvious that aspherical surfaces are widely used in miniature camera lenses. In fact, every surface in Table 1 except IR filters is aspheric, and notably, last two or three elements are usually highly aspherical.

Table 1 Representative design patterns of different element numbers.

(f: focal length, in mm; HFOV: half field of view, in degrees)

3-element	4-element		
A: US20140049840A1	B: US20120013998A1	C: US20140198397A1	D: US20150146308A1
$f = 1.53, F/2.75, \text{HFOV} = 33.0$	$f = 3.34, F/2.81, \text{HFOV} = 34.0$	$f = 2.22, F/2.20, \text{HFOV} = 33.7$	$f = 2.89, F/2.24, \text{HFOV} = 37.7$
5-element			
E: US20130258501A1	F: US20150022707A1	G: US20150316752A1	H: US20150077866A1
$f = 5.44, F/2.90, \text{HFOV} = 33.0$	$f = 3.97, F/2.20, \text{HFOV} = 37.68$	$f = 4.138, F/2.18, \text{HFOV} = 34.89$	$f = 4.109, F/2.20, \text{HFOV} = 35.6$

Table 1 -continued.

6-element			
I: US20140049843A1	J: US20150054994A1	K: US20160252711A1	L: US20160011405A1
$f = 3.66, F/2.20, \text{HFOV} = 38.0$	$f = 5.00, F/2.03, \text{HFOV} = 37.5$	$f = 3.02, F/2.40, \text{HFOV} = 37.1$	$f = 3.054, F/2.41, \text{HFOV} = 40.9$
7-element		8-element	
M: US20160341937A1	N: US20160033742A1	O: US20140376105A1	P: US9523841B1
$f = 4.01, F/2.00, \text{HFOV} = 44.3$	$f = 3.89, F/1.60, \text{HFOV} = 35.8$	$f = 6.76, F/2.4, \text{HFOV} = 41.2$	$f = 5.38, F/1.90, \text{HFOV} = 39.0$

A Quick Evaluation

To figure out the potential optimum designs in Table 1, four parameters W , S , CS , and AS are used as criteria¹². W and S are related to design patterns and often mentioned together. CS and AS describe tolerancing sensitivity and are grouped together.

W is the square root of the averaged and squared weighted powers of each surface in a lens. It describes the power distribution among optical surfaces. Small W means the lens efficiently uses the power of its surfaces and large W indicates surfaces contribute powers inefficiently. For aspherical surface, the optical power is calculated based on the axial curvature and regardless of the conic constant or high order aspherical coefficients.

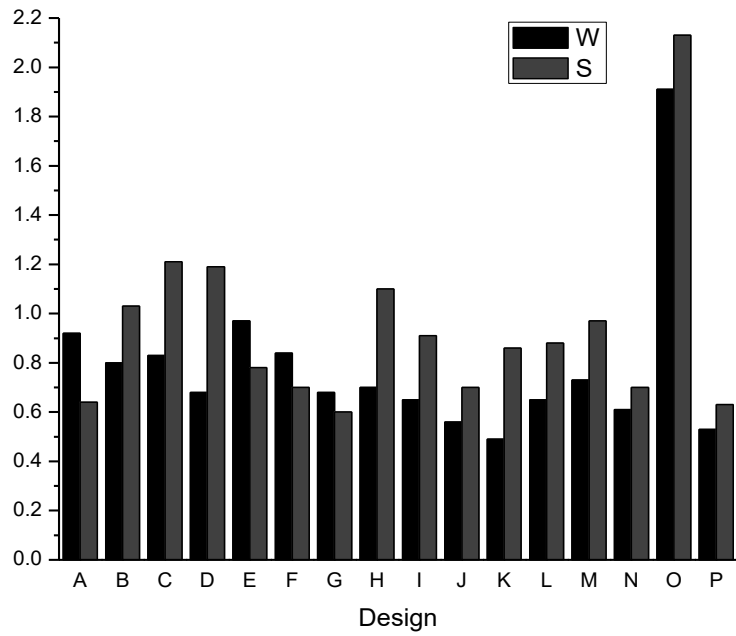
S is constructed in a similar way as W . It describes the lens symmetry. Because lens symmetry can help cancel or avoid some aberrations, it is also an important consideration in lens evaluation. Due to the requirement of incident ray angles on sensor, in miniature camera lenses, the stop is usually set as the first or front part, which is more or less against the element arrangement of symmetry³.

CS and AS represent coma and astigmatism sensitivity respectively. They describe the tolerancing sensitivity of a lens. All of the four parameters are independent of

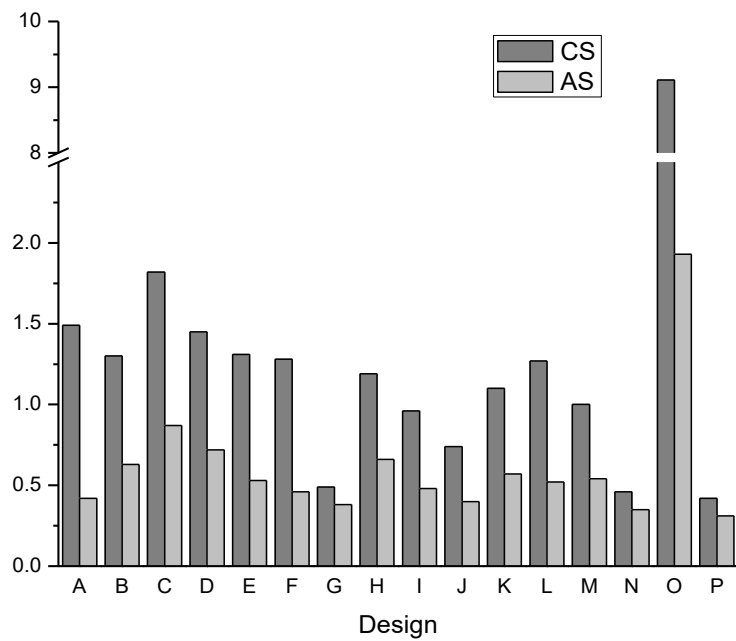
lens scaling, aperture size, field angle, or conjugation, which makes them a universal tool aiding in lens design and evaluation.

The calculations of W , S , CS , and AS are realized by macro files in lens design software and are applied to the sixteen designs in Table 1. The results are plotted separately in Fig. 6. In such a quick evaluation of multiple designs, CS and AS are also calculated based on the paraxial rays, which consist with W and S .

Though the main mechanism of sharp imaging is aberration cancellation, the four parameters still provide an inspection on the lens properties and prediction of lens performance. From Fig. 6, the potential optimum designs of each element number can be told, which are **G** for 5-, **J** for 6-, **N** for 7-, and **P** for 8-element, since all of their four parameters are less than 0.8. In contrast, **O** may not be a good design, because it has extraordinary high values of the four parameters.



(a)



(b)

Fig. 6 Parameters (a) W , S , (b) CS , and AS of sixteen lenses in Table 1

Two Relative Designs

Now that introducing more elements in lens design becomes a trend, to find out the possible differences made by doing so, two relative designs are compared. The selected two designs are from the hand of same two inventors, Tsung-Han Tsai and Hsin-Hsuan Huang from Largan Co. Fig. 7 are their layouts.

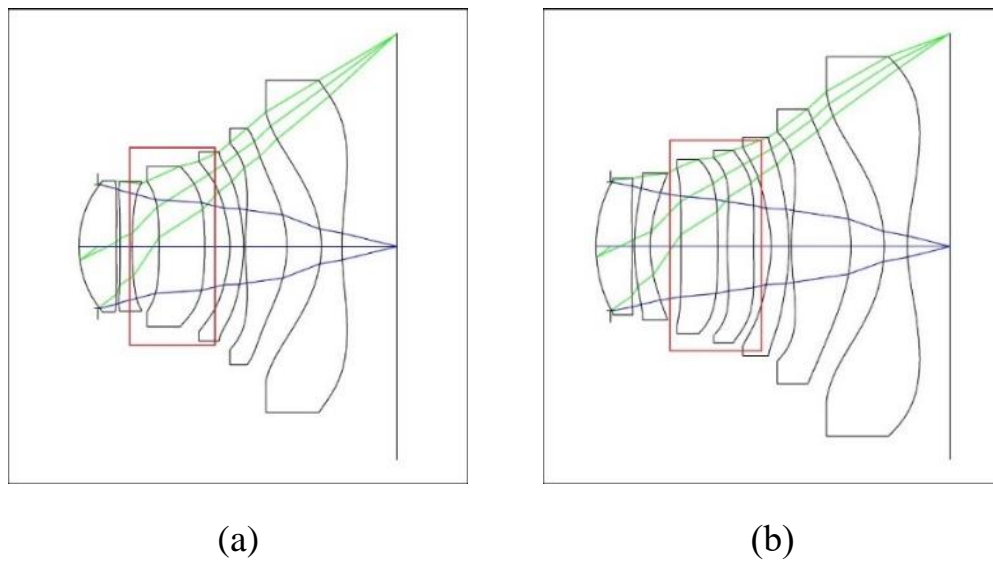


Fig. 7 Layouts of the selected (a) 6-element lens⁴ and (b) 7-element lens⁵

The lens design (a) in Fig. 7 is published on February 26th in 2015 and (b) is published later on November 24th in 2016. One can see that these two designs are almost the same, except the third element of (a) is split into two parts in (b) (in red boxes of Fig. 7). For conventional lens design, element splitting is a common method in controlling spherical aberration and other concerns. However, for the lens design adopting so many aspherical surfaces, which makes the nonlinearity

in imaging process go further, is the element splitting same useful in improving lens performance? Next, some primary analyses are made to answer.

Four Parameters Evaluation

Both of the lenses are reoptimized. The focal length after re-optimization of the 6-element lens (abbreviated as **6EL**) is 5.077 mm and of the 7-element lens (abbreviated as **7EL**) is 3.651 mm. To make the two lenses more comparable, the dimensions of 6-element lens is rescaled (abbreviated as **R6EL**) by factor 0.72 to have a focal length of 3.655 mm.

Firstly, we use the method of calculating four parameters introduced in last section to obtain a general evaluation of the two lenses. In such a case, *CS* and *AS* are calculated based on real ray tracing to makes the analysis closer to the real imaging process. Four parameters of the two lenses are tabulated in Table 2.

Table 2 Four parameters of the two compared lenses.

	R6EL	7EL
<i>W</i>	0.57	0.56
<i>S</i>	0.73	0.65
<i>CS</i>	0.0242	0.0122
<i>AS</i>	1.1240	0.0238
$(CS + AS) / 2$	0.5741	0.0180

From Table 2, we can see that their W are quite the same, which indicates that the efficiency of the two lenses using their elements are almost the same. The difference between their S is also not big. The absolute values of their CS are small, but that of **R6EL** is twice as large as **7EL**. AS of **7EL** is also small but that of **R6EL** is extraordinary large.

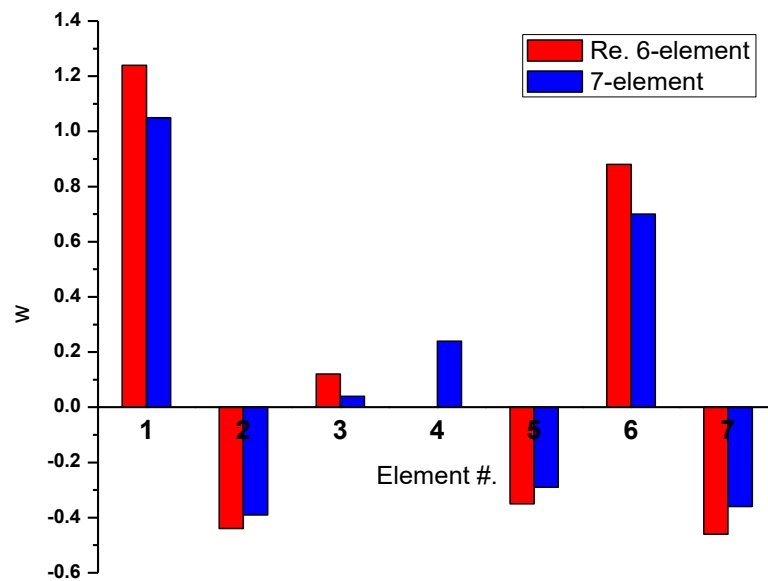


Fig. 8 Parameter w of each element of two compared lenses

To further illustrate the power distribution in the two lenses, w of each element of the two lenses are plotted in Fig. 8. To make a clear representation, the bars of 4th to 6th element of **R6EL** are lay back one spacing, so that each of them is next to the bars of 5th to 7th element of **7EL** respectively, since each pair have similar shapes and are thus comparable.

From Fig. 8, it can be seen that the power distribution of two lenses are quite similar, which implies that these two designs have intrinsic similarity. This is consistent with our first observation. For the 1st, 2nd, 5th, 6th, and 7th element pairs, w of **7EL** are all smaller than that of **R6EL**, except w of 4th element of **7EL** is bigger than that of the 3rd element of **R6EL**. Given that the summation of w for any lens is unity as it's constructed this way, the existence of the 4th element in **7EL** helps reduce the w values of the other elements, which is an obvious benefit of having more elements in lens design.

To make an element-by-element inspection on the tolerancing sensitivity, the average of cs and as of each element, providing an integral evaluation of sensitivity rather than solely focusing on coma or astigmatism sensitivity, are computed and plotted in Fig. 9.

From Fig. 9, we can see that the first element of each of the lenses has the dominating tolerancing sensitivity than the any element else does. This is corresponding to the fact that both of their first element has the most optical power distribution among others, which has been shown in Fig. 8.

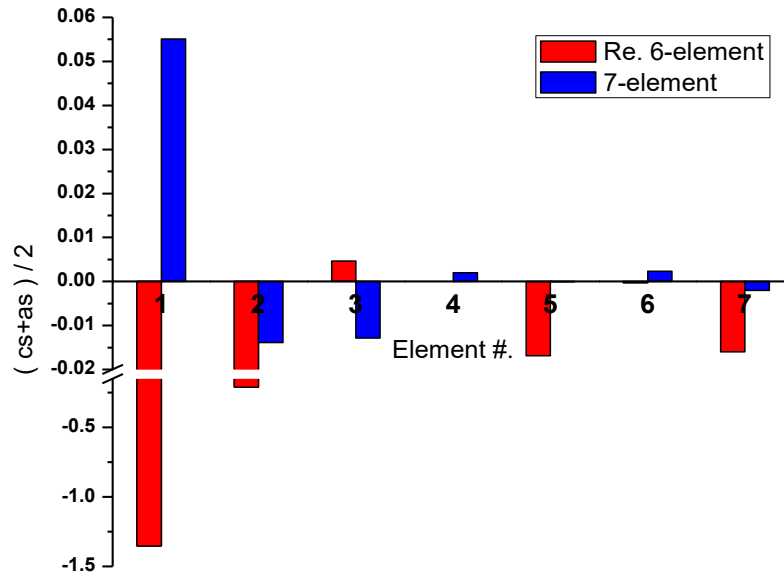


Fig. 9 Parameter $(cs + as) / 2$ of each element of two compared lenses

RMS Wave-front Error As Criterion

For lenses working near the diffraction limit, RMS wave-front errors are preferred as the criteria for evaluating imaging quality. RMS wave-front error reflects the uniformity of wave-front at exit pupil, and will not be remarkably influenced by local extremum. Smaller the RMS, smoother is the wave-front at exit pupil. Changes in RMS wave-front errors reflect the degradation in lens performance caused by perturbation.

As it has been mentioned, both of the lenses are reoptimized to have their RMS wave-front errors as close to zero as possible over the full field of view. In Fig.

10, RMS of **6EL**, **R6EL**, and **7EL** over +Y field are plotted due to the symmetry about X-Z plane. The reference wavelength is 587.6 nm.

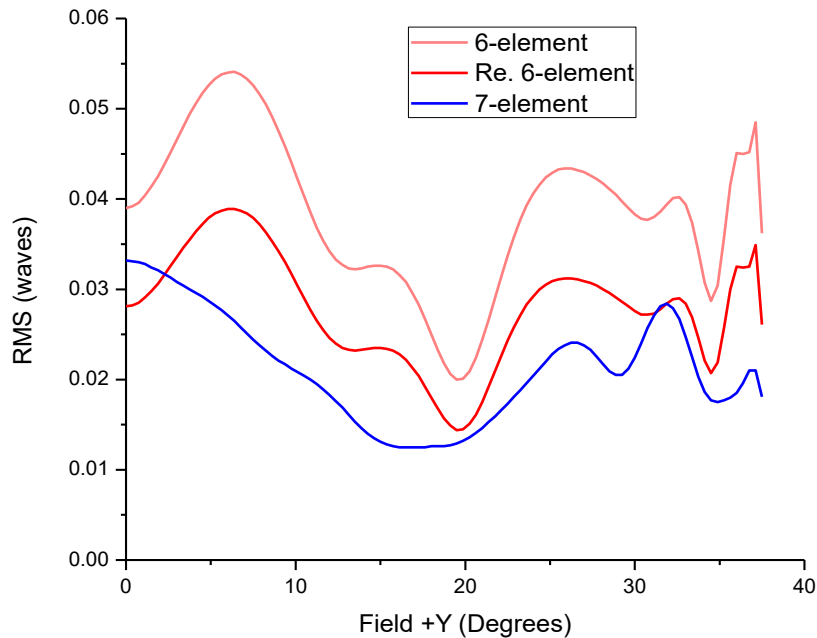


Fig. 10 RMS wave-front errors over HFOV

In Fig. 10, the blue line is totally beneath the light red line, which means **7EL** has a better overall optimizing result than **6EL**. However, the curvature changing of three lines are quite the same; that is their local maximum or minimum appears at same pace. This reflects the element arrangement of these two lenses has intrinsic similarity, and is another evidence of their relativeness. The RMS of **R6EL** is closer to that of **7EL**. The comparison will be made between them as before.

To further quantitatively compare the tolerancing sensitivity on the third element as a unity with that on two split elements, a couple of field points where the RMS changes will be observed are chosen. The first principle for choosing such kind of field points is that both of them should be where the local extremum shows up. This guarantees that these two field points have same imaging properties. The second is that their corresponding RMS should be close to each other, which makes the calculation results more comparable. In Table 3, three pairs of such kind of field points and their corresponding RMS are tabulated.

Table 3 Selected field points and the local RMS values.

(Field: in degrees; RMS: in waves)

Re. 6-element		7-element	
Field	RMS	Field	RMS
0	0.0271	0	0.0332
19.5	0.0160	18.75	0.0126
32.625	0.0317	31.875	0.0284

Point (0, 0.0271) and (0, 0.0332) in Table 3 are center field points and should be compared. (19.5, 0.0160) and (18.75, 0.0126) are both local minimum and close to each other. They could be treated as zonal field points. (32.625, 0.0317) and (31.875, 0.0284) are both local maximum and close to each other as well. They could be viewed as the edge field points.

Tolerancing By Element

For the two lenses, the third element of **R6EL** and third and fourth elements of **7EL** will be perturbed in the same manner, and the RMS changes at three selected field points will be observed. The third, fourth elements and the air gap in between of **7EL** are perturbed as a unity like a sandwich. The perturbation manners include element decentering along X and Y axis and tilting about X and Y axis in opposite directions.

The amplitude for element decentering is 0.003 mm and for tilting is 0.172 degrees, so that the amplitude of edge moving is also 0.003 mm according to the lens dimension⁶. The RMS changes with respect to different perturbances are tabulated in Table 4.

In Table 4, both of the absolute and relative RMS changes are listed. For each of the perturbation at different fields, the smaller relative RMS changes, that is also the better tolerancing performance, is marked bold and red for **R6EL**, blue for **7EL**.

According to Table 4, for the tolerancing sensitivity at center field, **7EL** is quite looser than **R6EL**. No matter what the perturbation is, the RMS of **7EL** at center field stays almost unchanged. However, for the zonal or edge field, neither **R6EL** nor **7EL** shows a prominent imaging stability in tolerancing. One lens may show

a loose tolerancing for some kinds of perturbation while the other may have more stable performance under other kinds of perturbation.

Table 4 RMS changes of different perturbances at three field points.

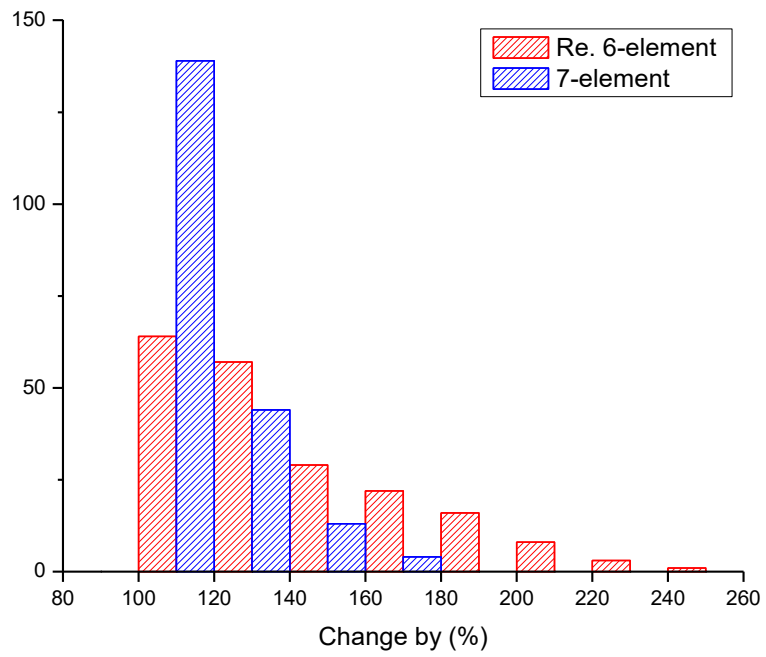
Fields	Lens Type	Re. 6-element		7-element	
	Element	3rd		3rd & 4th	
	RMS Changes	Δ	%	Δ	%
Center	Decenter +X	0.0161	59.41	0.0001	0.30
	Decenter -X	-	-	-	-
	Decenter +Y	0.0161	59.41	0.0001	0.30
	Decenter -Y	-	-	-	-
	Tilt +X	0.0145	53.51	0.0000	0.03
	Tilt -X	-	-	-	-
	Tilt +Y	0.0145	53.51	0.0000	0.03
	Tilt -Y	-	-	-	-
Zonal	Decenter +X	0.0177	110.63	0.0140	111.11
	Decenter -X	-	-	-	-
	Decenter +Y	0.0157	98.13	0.0397	315.08
	Decenter -Y	0.0221	138.13	0.0467	370.63
	Tilt +X	0.0428	267.50	0.0515	408.73
	Tilt -X	0.0438	273.75	0.0456	361.90
	Tilt +Y	0.0314	196.25	0.0215	170.63
	Tilt -Y	-	-	-	-
Edge	Decenter +X	0.0107	33.75	0.0053	18.66
	Decenter -X	-	-	-	-
	Decenter +Y	0.0722	227.76	0.0051	17.96
	Decenter -Y	0.0295	93.06	0.0357	125.70
	Tilt +X	0.0382	120.50	0.1053	370.77
	Tilt -X	0.0815	257.10	0.0549	193.31
	Tilt +Y	0.0184	58.04	0.0109	38.38
	Tilt -Y	-	-	-	-

Monte Carlo Analysis

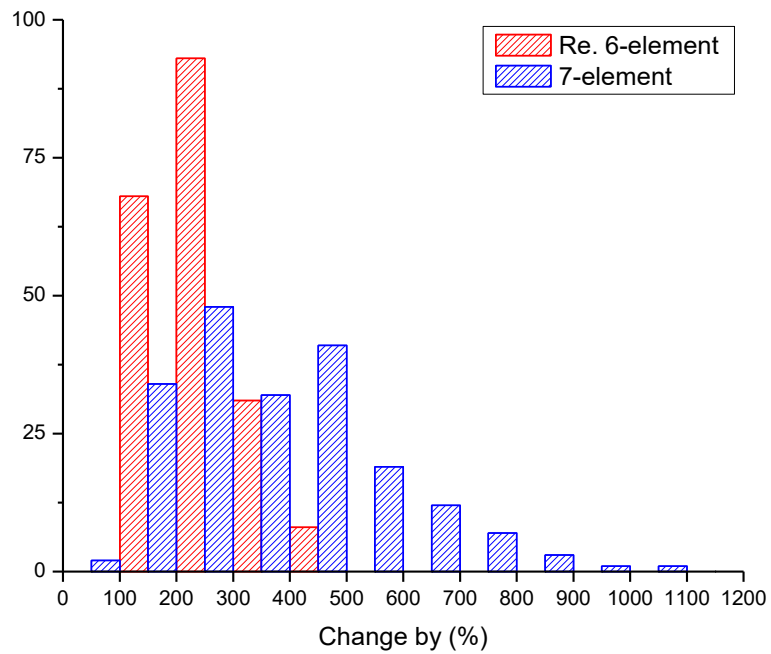
In real scenarios of application, the third and fourth elements of **7EL** may not and should not move as a unity. On the contrary, they may be moved by different kinds of perturbation in different amplitudes. To simulate this more actual circumstance, Monte Carlo analysis is needed.

Monte Carlo analysis will generate as many lenses as defined. For each lens, all of the tolerancing operands are randomly set using the defined value range and a statistical model of the distribution over the specified range⁷.

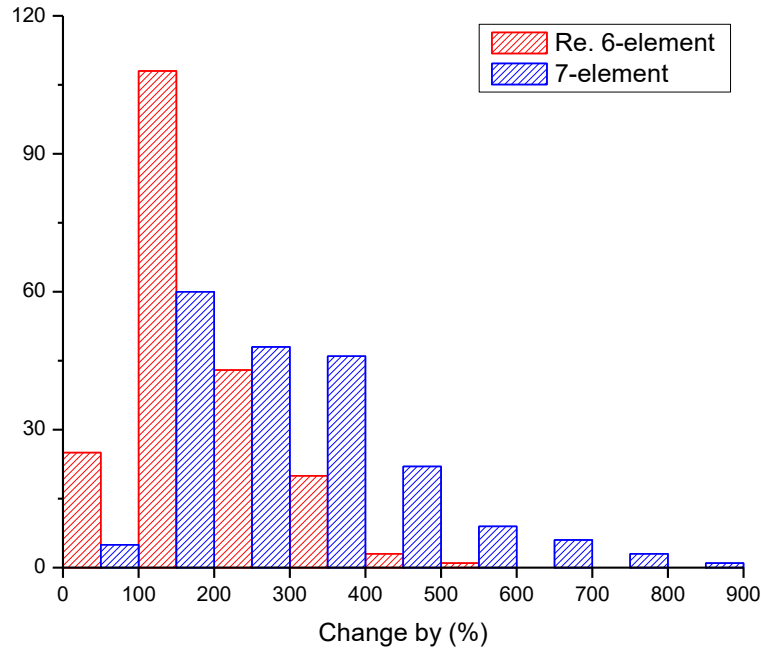
For our study, 200 perturbed lenses are generated for **R6EL** and **7EL** respectively. The kinds of perturbation are same as those listed in Table 4. The statistic model of tolerancing parameters is set as normal distribution. The histograms of changes of RMS wave-front errors by the initial values at center, zonal, and edge fields are plotted in Fig. 11. Mean and standard deviation for each figure are tabulated in Table 5.



(a) Center field



(b) Zonal field



(c) Edge field

Fig. 11 Histograms of RMS changes at (a) center, (b) zonal, and (c) edge fields

Table 5 Mean and standard deviation of Monte Carlo Analysis.

Field	Re. 6-element		7-element	
	Mean	S. Dev	Mean	S. Dev
Center	140.81%	31.73%	116.20%	14.76%
Zonal	242.25%	77.81%	375.63%	184.13%
Edge	182.84%	87.92%	297.85%	149.08%

From Fig. 11 and Table 5, we can find that for center field, both of mean and standard deviation of **7EL** are less than those of **R6EL**. However, for zonal and

edge field, both of mean and standard deviation of **R6EL** are smaller. This verifies the conclusion obtained in last section that **7EL** has a much more stable performance at center field than **R6EL** does. But for the zonal and edge field, Monte Carlo Analysis shows that **R6EL** performs better than **7EL**, which is not concluded in last section.

Conclusions

First of all, the trend of miniature camera lenses evolution is depicted by reviewing a large number of patents. In the past twenty years, the element number keeps increasing and the f-number keeps decreasing steady, which indicates the lenses become more sophisticated and faster. Other aspects of miniature camera lenses keep going various as the market demands is becoming diverse.

The representative design patterns having different numbers of elements are shown, of which the basic lens properties like focal length, F/#, and FOV are listed as well. Besides intuitive observation, a quick evaluation by calculating four parameters is also applied to the designs. The possible optimum designs of each element number are thus figured out.

Second, two relative designs published chronologically by the same inventors are picked out from a crowd of patents. The most significant difference of the two lenses is that the third element of the 6-element lens is split into two parts in the

7-element lens, which makes the third and fourth elements of the latter, leaving almost all of the other characters of the two lenses similar.

Next, we perturb the third element of 6-element lens and the third and fourth elements of 7-element lens in the same manners to observe the changes of RMS wave-front errors of each lens over the half field. In this part of study, the third and fourth elements of 7-element lens are perturbed as a unity. By this manual tolerancing analysis, it can be found that the 7-element lens has a much more stable performance at the center field than the 6-element lens. However, for the zonal and edge field, neither lenses show an obviously better tolerance than each other.

Finally, to analyze the tolerancing sensitivity on the third and fourth elements of 7-element lens separately, and to compare with that of the third element of 6-element lens, Monte Carlo analysis is applied to both lenses. The number of cycles of running Monte Carlo simulation is 200 and the statistic model of the amplitude of perturbation is normal distribution. As the result, the 7-element lens has a much more stable performance at the center field, which is coincide with the conclusion obtained in manual tolerancing analysis. However, for the zonal and edge field, 6-element lens has a better tolerance to the perturbances, which is not concluded in the manual analysis.

References

1. J. M. Sasián, M. R. Descour. “Power distribution and symmetry in lens systems.” *Optical Engineering*, **37**(3), 1001-1004 (1998).
2. L. Wang, J. M. Sasián. “Merit Figures for Fast Estimating Tolerancing Sensitivity.” International Optical Design Conference 2010. Proc. SPIE-OSA 7652, 76521P (2010).
3. T. V. Galstian. *Smart Mini-Cameras*. CRC Press, 2013.
4. U.S. Patent No.: 2015/0054994 A1.
5. U.S. Patent No.: 2016/0341937 A1.
6. R. Bates. “Performance and Tolerance Sensitivity Optimization of Highly Aspheric Miniature Camera Lenses.” Optical System Alignment, Tolerancing, and Verification IV. Proc. SPIE 7793, 779302 (2010).
7. OpticStudio® 16.5 SP3 Help Files.